

UV-visible photodegradation of naproxen in water – Structural elucidation of photoproducts and potential toxicity

European Journal of Mass Spectrometry
2020, Vol. 26(6) 400–408
© The Author(s) 2020



Article reuse guidelines:
sagepub.com/journals-permissions
DOI: 10.1177/1469066720973412
journals.sagepub.com/home/ems



Noemi Cazzaniga, Zsuzsanna Varga, Edith Nicol and Stéphane Bouchonnet 

Abstract

The UV-visible photodegradation of Naproxen (6-methoxy- α -methyl-2-naphthaleneacetic acid, CAS: 22204-53-1), one of the most used and detected non-steroidal anti-inflammatory drugs (NSAIDs) in the world, and its ecotoxicological consequences were investigated in an aqueous medium. The photo-transformation products were analyzed and the structures of photoproducts were elucidated using gas chromatography coupled with tandem mass spectrometry (GC-MS/MS) and high-performance liquid chromatography coupled with ultrahigh-resolution Fourier transform ion cyclotron resonance mass spectrometry (LC-FTICR-MS). Seven photoproducts were detected and characterized, photo-transformation mechanisms have been postulated to rationalize their formation under irradiation. *In silico* Q.S.A.R. (Quantitative Structure-Activity Relationship) toxicity predictions were performed with the Toxicity Estimation Software Tool (T.E.S.T.) and *in vitro* assays were carried out on *Vibrio fischeri* bacteria. Some of the obtained photoproducts exhibit higher potential toxicity than Naproxen itself but the whole toxicity of the irradiated solution is not of major concern.

Keywords

Naproxen, photodegradation, structural elucidation, toxicity, mass spectrometry

Received 27 August 2020; accepted 24 October 2020

Introduction

As the human body does not break them down entirely, pharmaceuticals and their metabolites represent a significant source of environmental contamination and their ever-increasing consumption is a major issue for the environment and human safety. The volume of medicines used globally will reach 4.5 trillion doses by the end of 2020 on a 1.4 trillion dollar market.¹ Frequent use and active consumption of pharmaceuticals led to increased levels of drug-related residues in the environment. More than 600 active pharmaceutical ingredients (APIs) or their metabolites and photo-degradation products have been identified, mainly in surface water and wastewater, but also in groundwater, soil, and other environmental matrices.² High concentrations of pharmaceutical products reach wastewater treatment plants (WWTP), mainly through human urinary, fecal excretion, and industrial discharges, and a considerable variety of drugs is not mineralized by conventional treatment processes. It is now turned out that hospital effluents are also significant sources of aquatic environmental pollution.³ Consequently, more and more research is devoted to design specific

pilot plants suitable for the degradation of biocides and drugs in hospital effluents, aiming at reducing the pharmaceutical burden of wastewater treatment plants and the associated risk.

In the past years, different prioritization approaches, based on consumption data, experimental toxicological and physicochemical data, and *in silico* predictions, were carried out to screen and identify the most environmentally hazardous pharmaceuticals. A recent study using a QSAR (Quantitative Structure-Activity Relationship) approach has shown that pharmaceutical products constitute a new generation of contaminants of emerging concern that can affect wildlife and the ecosystem even at low concentrations.⁴ The majority (83%) of the drugs screened were predicted to be non-PBT (Persistent, Bioaccumulative, Toxic) and therefore, may not be

Laboratoire de Chimie Moléculaire – CNRS/Ecole polytechnique, Institut Polytechnique de Paris, Palaiseau, France

Corresponding author:

Stéphane Bouchonnet, Laboratoire de Chimie Moléculaire – CNRS/Ecole polytechnique, Institut Polytechnique de Paris, 91128 Palaiseau, France.
Email: stephane.bouchonnet@polytechnique.edu

considered dangerous for the ecosystem. 35 drugs have been identified as potential PBTs, for which an experimental evaluation will have to be made to confirm the expected PBT behavior.^{5,6}

Contrary to chronic toxicity, the acute toxicity of nonsteroidal anti-inflammatory drugs (NSAIDs) has not been widely studied, except in the case of propranolol, which shows high acute toxicity. 17% of the medicines exhibited human LC50 values lower than 100 mg/L, which according to EU Directive 93/67/EEC⁷ correspond to acute toxicity, 38% exhibited LC50 values above 100 mg/L and were thus classified as not harmful to aquatic organisms. The remaining 45% showed a considerable variability of acute toxicity values depending on the way they were evaluated. In the case of Naproxen, the provided EC50 values fall in a range as wide as 10-1000 mg/L.^{8,9}

According to statistics conducted in 2017 on clinical drugs, Naproxen was the 71st most prescribed medication in the United States, with more than eleven million prescriptions. It belongs to the priority list of substances defined by the Global Water Research Coalition (GWRC, 2008);¹⁰ it is also on the list of contaminants of emerging concern compiled by the NORMAN network, specialized in monitoring and biomonitoring of emerging environmental substances.¹¹ Naproxen is one of the most commonly detected pharmaceutical compounds in the environment, with concentrations in surface waters up to 32 µg/L.⁹ It is mainly excreted in urine (95% of the quantity ingested) and is not effectively removed by current wastewater treatments. A Naproxen concentration of 6 µg/L has been reported in raw urban wastewater and effluent from a system of activated sludge, a common treatment adopted for urban wastewaters prior to final discharge into surface water bodies.¹² In another study conducted on raw urban wastewater and effluent from an activated sludge system, Ibuprofen was detected at the highest concentration (373 µg/L), followed by Naproxen (53 µg/L). No significant reduction was found for Ibuprofen and Naproxen in the pre-treatment and sedimentation step; because of their acidic structures and their very low solid-liquid partition K_d coefficients, both molecules undergo very poor sorption onto sludge and mainly remain in the aqueous phase.¹³

It has been demonstrated that Naproxen, by itself or through its metabolites, can affect organisms that inhabit ecosystems and one of the most important aspects of studies on the degradation of pollutants is the toxicity of degradation products, which in some cases can be higher than that of the parent molecule.¹⁴ The main objective of the present work was to characterize the photoproducts generated from direct photolysis of Naproxen, based on GC-MS and LC-MS investigations. Ultra-high-resolution measurements permitted direct assignment of exact formulae

while tandem experiments allowed structural elucidation for the major part of photoproducts. The second aim of this work was to estimate the potential toxicity of the photoproducts using both *in silico* (QSAR calculations) and *in vitro* (luminescence inhibition tests on *Vibrio fischeri* marine bacteria) approaches, to determine whether UV-visible photodegradation could be an efficient solution for the safe removal of Naproxen, for instance from hospital effluents.

Experimental

Chemicals and reagents

Naproxen (6-methoxy- α -methyl-2-naphthaleneacetic acid, CAS: 22204-53-1) was provided by Sigma Aldrich (Madrid, Spain). Acetonitrile (ACN), methanol and dichloromethane (Sigma Aldrich, Saint Quentin Fallavier, France) were of chromatographic grade, i.e. with purity > 99.99%. BSFTA (N,O-Bis(trimethylsilyl)trifluoroacetamide) and formic acid were also from Sigma Aldrich (Saint Quentin Fallavier, France). Ultra-pure water (conductance of 18.2 S/cm) was obtained purifying tap water with a Purelab Chorus 1 system (Veolia, Wissous, France).

Sample preparation

Naproxen solutions were prepared at four concentrations: 2, 10, 100, and 500 ppm in water to which 0.1% acetonitrile was added regarding the poor solubility of Naproxen in pure water close to neutral pH (around 4 mg/L at 25 °C according to the Henderson-Hasselbach equation). Different irradiation times were tested, to determine the appearance order of photoproducts. The solutions were irradiated up to a maximum of 6 hours with sampling at t 0-2-5-10-15-30-45-60-80-100-120 minutes, then every thirty minutes up to the fourth hour and every hour until the end of the analysis. For GC-MS analysis, all samples were dried using an Xcelvap automated evaporation/concentration system (Biotage, Uppsala, Sweden) for an hour, then put in an oven (WTC Binder 7200, Tuttlingen, Germany) for 10 minutes at 80 °C to remove any trace of water. Silylation was achieved adding 100 µL of BSTFA (N,O-Bis(trimethylsilyl) trifluoroacetamide) and placing the sample in the oven for 30 minutes. 100 µL of dichloromethane (DCM) was added prior to GC-MS analysis to reconstitute the sample. For LC-MS coupling measurements, samples were dissolved in ultrapure water to reach a final concentration of 2 ppm for non-degraded Naproxen at t_0 . For HRMS analysis in direct infusion mode, samples were diluted in a mixture of H₂O/ACN/FA 90/10/0.1%, to reach a 2 ppm concentration for Naproxen at t_0 . All samples were stored sheltered from light at 4 °C.

Photolysis experiments

Photodegradation experiments were conducted using a home-made photoreactor equipped with a high-pressure mercury lamp HPL-N 125W/542 E27 SC (Phillips, Ivry-sur-Seine, France) that emits light on wavelengths between 200 nm and 650 nm, with maximum irradiation at 254 nm and a radiation flow of 6200 lm. The lamp is located in a quartz tube at the center of an AL04-12 sonicator (Advantage-Lab GmbH, Darmstadt, Germany) and samples are placed in quartz tubes around, at equal distance to the lamp. The sonicator is used to achieve the solubilization of compounds before irradiation. To avoid thermal degradation, the temperature was manually adjusted to $30 \pm 5^\circ\text{C}$ flowing cold-water through the sonicator manifold.

GC-MS operating conditions

Gas chromatographic separations were carried out on an Agilent 7890B GC instrument equipped with a 30 m HP-5MS column (5% Phenylmethylpolysiloxane) with an internal diameter of 0.25 mm and film thickness of 0.25 μm , coupled with an Agilent 7000 D GC/TQ triple quadrupole mass spectrometer (Agilent Technologies, Les Ulis, France). Samples were injected in splitless mode using an Agilent 7693 A autosampler, the injection volume was 1 μL and injector temperature was 280°C . A gradient temperature program was used with an initial temperature of 50°C , held for 0.5 min then increased to 320°C with a ramp of $20^\circ\text{C}/\text{min}$. The carrier gas was high purity helium, with an autor-regulated flow of 1.2 ml/min. Measurements were carried out in electron ionization (70 eV) with a filament emission current of 35 μA . The electron multiplier voltage was automatically optimized at 1090 V, for a gain value of 10^5 . In the full scan mode, ions were scanned from m/z 50 to m/z 600. Tandem experiment measurements were performed, using argon as the collision gas, with collision energies of 15, 30, and 45 eV. The source temperature was set to 230°C .

LC-MS operating conditions

Chromatographic separations were carried out using an Acquity HPLC system (Waters Technologies, Guyancourt, France) equipped with a C_{18} Pursuit XRs Ultra 2.8 μm , 50×2.0 mm column (Agilent Technologies, Les Ulis, France) and coupled with an FT-ICR SolarixXR 9.4T (Bruker Daltonics, Bremen, Germany). The injection volume was 10 μL , elution was performed using a 0.1 mL/min flow with a mixture of solvents A (water, formic acid 0.1%) and B (acetonitrile, formic acid 0.1%). After 10 minutes, the percentage of solvent B was increased from an initial value of 5% to 40% in 15 min, then to 90% in 5 min. The gradient was

then set back to initial conditions (5% of B) during the last 20 min, for a total method duration of 50 min. An electrospray ionization source was used both in positive and negative mode, the nebulizer and drying gas was nitrogen with a flow of 8 L/min at 250°C for drying gas and 1 bar for nebulizer gas. The capillary voltage and end plate offset values were set to -4500 V and -4000 V, respectively for positive mode, and 3000 V and 2500 V, respectively for negative mode. Argon was used as the collision gas for tandem experiments. Ions were accumulated in the collision cell for 0.2 s in MS experiments and 2 s in MS/MS experiments. The ion detection mode was set to 4 Mpt with a 0.8389 s transient duration in broadband mode from m/z 57.7 to m/z 1000 to obtain a resolution higher than 350 000 at m/z 200. To reduce the size of the data file, 97% of the data (contributing to noise) were not recorded to get a data file size below 2 GB per analysis. Phosphoric acid was used for external mass calibration and exact chemical formulae were attributed with tolerance below 3 ppm. For tandem MS experiments, precursor ions were isolated with an isolation window of 1 m/z and dissociated, using argon as the collision gas, with collision energies of 10, 15, 20, and 25 V to study the fragmentation mechanisms.

In silico toxicity estimations

The toxicities of Naproxen and its photoproducts were *in silico* evaluated regarding developmental toxicity, oral rat LD50 (mg/kg), and Fathead minnow LC50 (96 h) (mg/L). The Toxicity Estimation Software Tool (T.E.S.T.) - based on Quantitative Structure-Activity Relationship (QSAR) mathematical models - was used for this purpose.¹⁵ T.E.S.T. has been developed by the U.S. Environmental Protection Agency, its main features are briefly described in Supplementary information SI-1.

In vitro bioassays

Vibrio fischeri commercial *in vitro* test kit was used to evaluate the global ecotoxicity of solutions before (initial concentration of 50 $\mu\text{g}/\text{L}$ in Naproxen) and after two times of irradiation: 30 and 80 min. The freeze-dried luminescent bacteria and the luminometer were purchased from Hach Lange (GmbH, Düsseldorf, Germany). The experimental method used in this study is based on the ISO 11348-3 protocol.¹⁶ Luminescence was measured in duplicate before the addition of the test solution and after contact times of 5, 15, and 30 min; results were corrected using the values measured with control samples. The effective nominal concentration leading to 20% inhibition of bioluminescence is designated as the EC20.

Results and discussion

Kinetics of photoproducts and degradation efficiency

The relative concentration of Naproxen in ultrapure water was followed by LC-MS over the irradiation time (6 hours), integrating the area of the corresponding chromatographic peak on the $[M + H]^+$ ion. The initial amount of Naproxen (initial concentration of 2 ppm) was halved after about 30 minutes and the compound was no longer detected after 45 minutes. In order to correlate the appearance of some photoproducts with the disappearance of some others, their relative abundances (normalized data from GC-MS and LC-MS signals) were plotted as a function of irradiation time (Figure 1). Photoproducts are referred as PP1 to PP7; their structures are given in Tables 1 and 2.

To compare the relative amounts estimated by GC-MS and LC-MS couplings, LC-MS peak areas were corrected by a factor determined on the basis of the peak areas of Naproxen detected by both techniques at t_0 . This empirical approach aimed at making possible a rough comparison between ion abundances from both techniques; it did not serve a quantification purpose, but allowed to discriminate reaction intermediates from photoproducts likely to be found under real sunlight degradation. Seven photoproducts were determined. After a few minutes of irradiation, **PP6** is by far the most abundant before **PP1**. Furthermore, **PP6** appears as the only persistent compound at the end of the experiment while all the other photoproducts appear as reaction intermediates. Correlating their relative appearance and disappearance order helped to assign their chemical structures (see section 3.2).

Structural elucidation of photoproducts

GC-MS experiments allowed the structural elucidation of photoproducts **PP1** to **PP3**; retention times, ions, and chemical structures are given in Table 1. Dissociations of molecular ions were interpreted; the silylated compounds were easily identified due to the presence of a fairly intense ion at m/z 73 ($\text{Si}(\text{CH}_3)_3^+$) in their mass spectrum. Dissociation mechanisms of molecular ions are provided in Supplementary information SI-2.

The retention times and m/z measured for protonated and deprotonated species in LC-ESI-MS are given in Table 2. Collision induced experiments permitted the structural elucidation of the photoproducts. Transitions and associated mechanisms are provided in Supplementary information SI-3 and SI-4.

Based on the chemical structures of photoproducts, a photodegradation mechanism of naproxen has been proposed, which involves classical

photochemistry pathways such as Norrish-type cleavage, hydrogen abstraction, oxygen addition (from water dissolved oxygen), hydrolysis, and concerted eliminations (see Figure 2). As is often the case with ketones, the photodegradation process begins by the Norrish-type cleavage of the C-CO bond of naproxen, leading to a radical which, in contact with a water molecule, can abstract a hydrogen atom or a hydroxyl group to lead to **PP1** and **PP2**, respectively. Photo-induced cleavages of C-H bonds have been recently demonstrated in a study by De Vaugelade et al. reporting the UV-Vis photodegradation of alpha-tocopherol.¹⁷ Cleavage of such bonds is only observed if the resulting radical is strongly stabilized by mesomeric and/or inductive effects, which is the case when removing the hydrogen atom carried by the same carbon atom than the hydroxyl group in **PP2**. The resulting radical can lose a second hydrogen atom to lead to the ketone **PP3**. Successive oxygen additions on **PP3**, combined with hydrolysis reactions lead to **PP6**, then to **PP5**. By analogous mechanisms, the consecutive oxidation and hydrolysis of **PP3** leads to **PP4**. Quite surprisingly, **PP7** results from methanol elimination from naproxen, followed by hydrogen addition, the hydrogen atom is abstracted from a water molecule. This type of mechanism is not “classical” in photochemistry but both the structure of naproxen and the MS dissociation pathways of **PP7H⁺** allow unambiguous identification of the latter.

In silico and in vitro toxicity estimations

In silico toxicity estimation. QSAR in silico tests were carried out with the T.E.S.T. software (see Supplementary information SI-1) regarding development toxicity, oral rat LD50 (mg/kg), and Fathead minnow LC50 (96 hours) (mg/L); results are presented in Table 3.

Considering developmental toxicity, all compounds except **PP4** are potentially toxic, the latter having a toxicity value coefficient of 0.37, which is below the threshold of toxicity value (0.50); they are expected to be at least as toxic as Naproxen. Regarding oral rat toxicity, the values reported in Table 3 show that all photoproducts are in category III (slightly toxic) at the exception of **PP7** which belongs to category II corresponding to moderate toxicity. The higher toxicity of **PP7** compared to other photoproducts is quite close to that of Naproxen; this is consistent with the fact that the chemical structure of **PP7** is the closest to that of the parent molecule. The lowest LC50 values were determined for **PP5** and **PP6**, which exhibit the most hydrophilic structures and thus the lowest potentials for bioaccumulation. An oral rat LD50 experimental value of 248 mg/kg was provided for Naproxen, which is comparable but below the

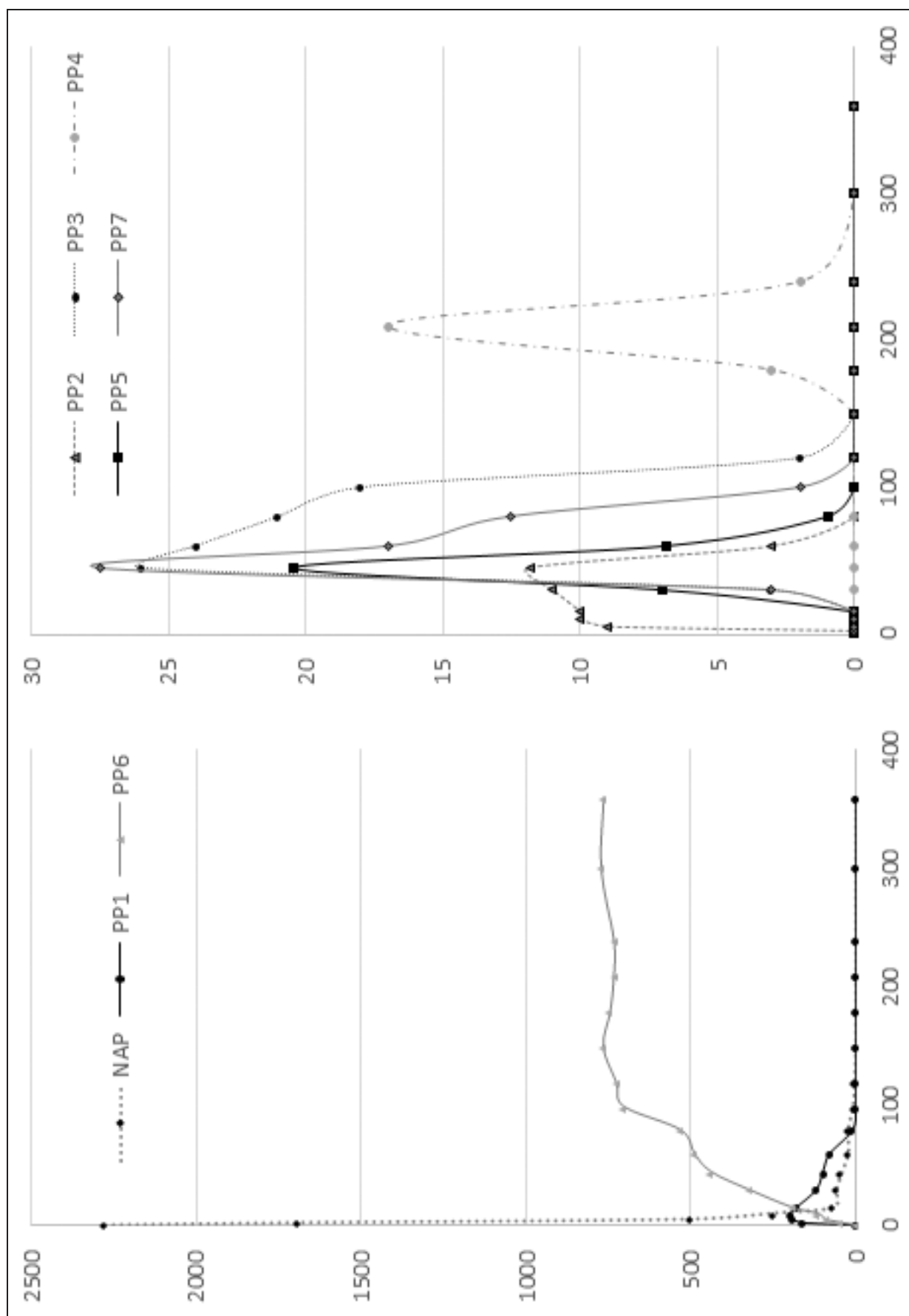
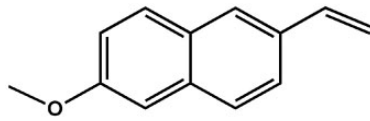
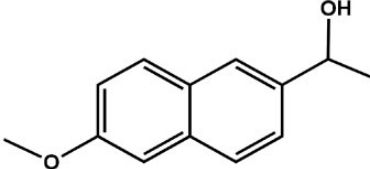
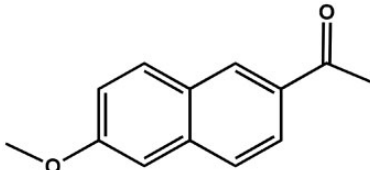
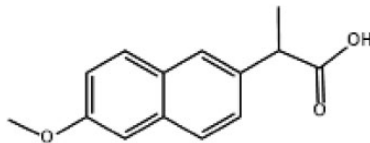


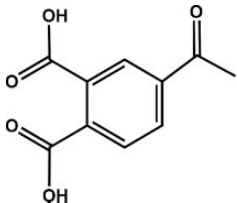
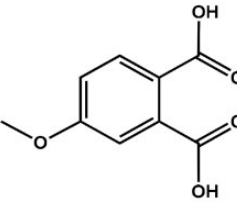
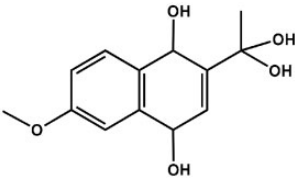
Figure 1. Relative abundances of Naproxen and its photoproducts over time: compounds of major abundances (NAP, PP1, and PP6) on the left side and compounds of minor abundances (PP2, PP3, PP4, PP5, and PP7) on the right side. On the y-axis, abundances are normalized to that of Naproxen at t_0 . The x-axis corresponds to the irradiation time in minutes.

Table 1. Retention times, main ions, and elucidated structures of the photoproducts **PP1** to **PP3** detected in GC-MS/MS (electron ionization).

Ret. time (min)	Compound	Silylated	Main ions in MS/MS (m/z) – precursor in bold ^a	Photoproduct
9.08	PP1	No	184 , 169, 141, 115	
10.12	PP2	Yes	274 , 259, 185, 141, 73	
10.18	PP3	No	200 , 185, 158, 157, 128	
11.00	Naproxen	Yes	302 , 287, 243, 185, 73	

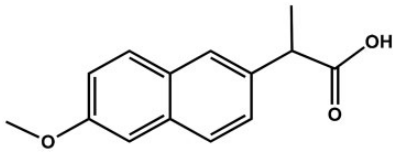
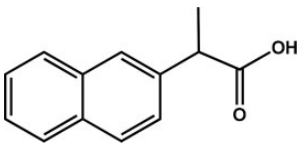
^aNote that the provided m/z values correspond to ions from the silylated structure in the case of derivatized compounds, i.e. PP2 and Naproxen. For both compounds, the molecular mass of the photoproduct and thus that of the molecular ion are shifted by 72 amu since the OH function has been replaced by OSi(CH₃)₃.

Table 2. Retention times, main ions, and elucidated structures of the photoproducts **PP4** to **PP7** detected by LC-ESI-MS.

Ret. time (min)	Compound	Detection in ESI+		Detection in ESI-		Structure of the compound
		MH ⁺ ion (m/z)	MH ⁺ formula	MH ⁻ ion (m/z)	MH ⁻ formula	
7.51	PP4	209.04502	C ₁₀ H ₉ O ₅ ⁺	207.02990	C ₁₀ H ₇ O ₅ ⁻	
8.26	PP5	197.04475	C ₉ H ₉ O ₅ ⁺	195.03025	C ₉ H ₇ O ₅ ⁻	
8.72	PP6	253.10742	C ₁₃ H ₁₇ O ₅ ⁺	251.09250	C ₁₃ H ₁₅ O ₅ ⁻	

(continued)

Table 2. Continued

Ret. time (min)	Compound	Detection in ESI+		Detection in ESI-		Structure of the compound
		MH ⁺ ion (m/z)	MH ⁺ formula	MH ⁻ ion (m/z)	MH ⁻ formula	
13.00	Naproxen	231.10198	C ₁₄ H ₁₅ O ₃ ⁺	-	-	
13.14	PP7	201.09152	C ₁₃ H ₁₃ O ₂ ⁺	-	-	

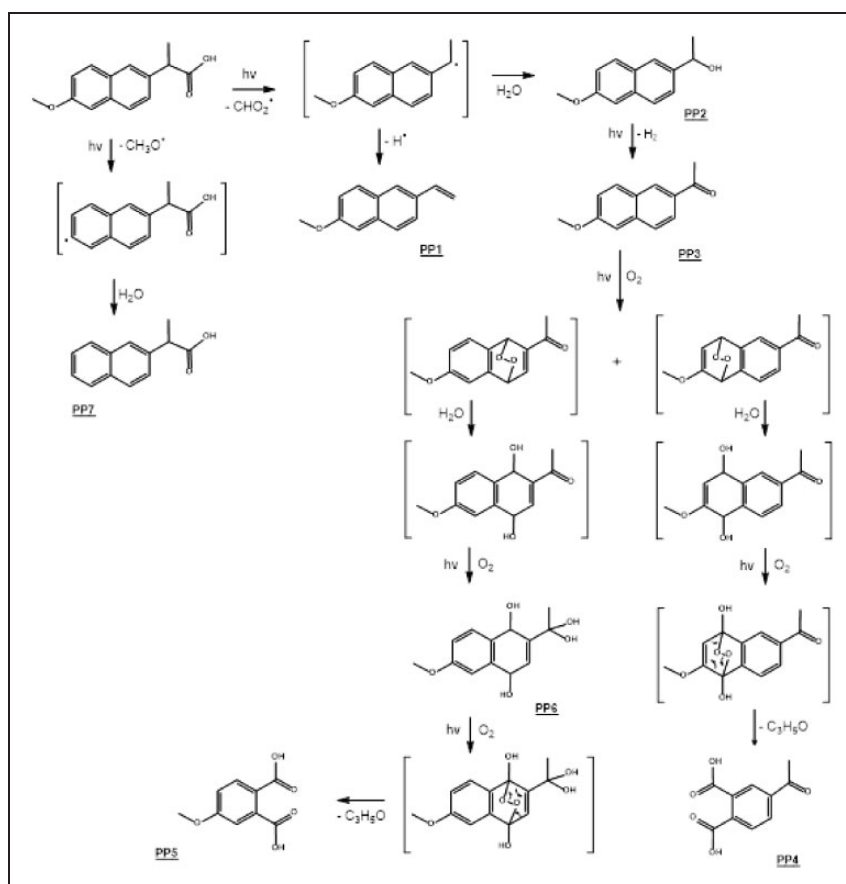


Figure 2. Mechanisms proposed for the photodegradation of Naproxen in water.

estimated one (516 mg/kg).¹⁸ Nevertheless, it suggests that the *in-silico* approach used could underestimate the toxicity of Naproxen and its photoproducts due to the lack of experimental data on similar structures. Regarding the toxic effect on Fathead minnow, **PP1** exhibits by far the highest potential toxicity, in agreement with previous results.¹⁹ **PP2**, **PP3**, and **PP7** provide LC50 values close to that of the parent compound. The specificity of **PP1** is that it does not include any CO nor OH group, which makes it much

less polar than other compounds. Here again, the most hydrophilic compounds exhibit the lowest potential toxicity. In a previous study on UV photodegradation of Naproxen by Cory et al., only **PP2** and **PP3** were detected though the experimental conditions were quite similar to those used in the present work.²⁰ Like in the present study, both photo-transformation products of Naproxen were found to be more stable than Naproxen itself when exposed to simulated sunlight; their toxicity was investigated

Table 3. Toxicity values estimated by the T.E.S.T. software for Naproxen and its photoproducts.

Compound	Fathead		Developmental toxicity value ^a	Developmental toxicity
	Minnow LC50 (96 h) (mg/L)	oral rat LD50 (mg/kg)		
NAP	5.3	515.5	0.89	Toxicant
PP1	0.2	667.8	0.53	Toxicant
PP2	5.5	1817.9	0.85	Toxicant
PP3	6.6	1594.0	0.51	Toxicant
PP4	22.8	4230.5	0.37	Non-toxicant
PP5	69.9	3913.9	0.69	Toxicant
PP6	19.4	1661.8	0.52	Toxicant
PP7	6.8	311.7	0.96	Toxicant

^aArbitrary unit.

towards toad tadpoles and they have been shown to be much more toxic than the parent molecule.

In vitro toxicity estimation. *In vitro* bioassays based on the bioluminescence extinction of *Vibrio fischeri* were carried out on the solution of Naproxen at different irradiation times according to the protocol described in section 1.7. Unlike *in silico* testing, this approach takes into account potential mixture effects. In the above-mentioned protocol, estimation of an EC50 value requires a minimum of three measurements for which the inhibition is between 10% and 90%, with a value above 50% for at least one of the three measurements. A Naproxen solution at 50 ppm was submitted to photodegradation; sampling was performed at t_0 , t_{30} , and t_{80} (minutes). For each sample, the conditions were not met for EC50 determination, indicating a low ecotoxicity; an EC20 was thus evaluated, based on linear regression analysis of the dose-effect relationship. For a duration exposure of 15 minutes, the EC20 value decreases when increasing the irradiation time, from 11.7 at t_0 to 7.2 at 80 minutes, which traduces a slight increase in toxicity of the mixture. As shown in Figure 1, **PP6** is by far the most abundant photoproduct in the mixture at 80 minutes. Regarding *in silico* estimations, **PP6** exhibits Fathead Minnow LC50 and oral rat LD50 values higher than those estimated for Naproxen so this photoproduct is not *a priori* expected to contribute to the increase in toxicity of the mixture. Different conclusions can be drawn from these estimations: (i) insufficient parametrization of the T.E.S.T. software regarding the molecules of interest makes the *in silico* estimations inaccurate in the present case, especially in the case of **PP6**, which displays a quite complex and unusual structure; (ii) with a Fathead Minnow LC50 estimated to be 25 times lower than that of Naproxen (see Table 3), **PP1**, which is the second photoproduct in terms of abundance, could be responsible for the slight increase in toxicity of the mixture; (iii) a limited “cocktail effect” due to the concomitant presence of several photoproducts

could also be suspected. Whatever the right explanation, both *in silico* and *in vitro* evaluations lead to the outcome that the ecotoxicity induced by Naproxen photoproducts is not a major issue compared to that of Naproxen itself. However, the long-term environmental effects of Naproxen exposure at concentration levels close to those found in the environment remain poorly studied although detection of the drug in wastewater and river samples in the ng/L - µg/L range demonstrated the need for such knowledge.^{21–23}

Conclusion

The in-lab photodegradation of Naproxen under UV-Visible irradiation led to the formation of seven photoproducts, which were characterized using LC-HR-MS/MS and GC-MS techniques. A photodegradation pathway of Naproxen has been suggested based on the elucidated structures and kinetics considerations. *In silico* and *in vitro* tests were conducted, on isolated molecules in the first case, on an irradiated aqueous solution of Naproxen in the second one. The general conclusion is that photoproducts do not increase the global toxicity in an alarming way. It is interesting to note that Naproxen was 90% degraded after only a few minutes and that all the photoproducts are eliminated after 5 hours of irradiation with the exception of **PP6**, which remains in the mixture in significant amounts and whose toxicity would deserve to be further investigated after synthesis. Aside from the consequences of sunlight-induced degradation of Naproxen in the environment, these results suggest that direct UV light irradiation – a technique gradually replacing the more classical photocatalytic processes – could be an efficient tool for Naproxen removal from contaminated waters.

Declaration of conflicting interests

The author(s) declared no potential conflicts of interest with respect to the research, authorship, and/or publication of this article.

Funding

The author(s) disclosed the receipt of the following financial support for the research, authorship, and/or publication of this article: Financial support from the National FT-ICR network (FR 3624 CNRS) for conducting the research is gratefully acknowledged. This work is part of a project that has received funding from the European Union’s Horizon 2020 research and innovation program under the Marie Skłodowska-Curie Grant Agreement No 765860 (AQUALity).

ORCID iD

Stéphane Bouchonnet  <https://orcid.org/0000-0003-2636-1093>

Supplemental material

Supplemental material for this article is available online.

References

1. Verlicchi P, Al Aukidy M and Zambello E. Occurrence of pharmaceutical compounds in urban wastewater: removal, mass load and environmental risk after a secondary treatment – a review. *Sci Total Environ* 2012; 429: 123–155.
2. European Environmental Bureau. The environmental and health impacts caused by emissions of APIs to the environment, file:///C:/Users/STEPAN~1/AppData/Local/Temp/Comment-The-environmental-and-health-impacts-caused-by-emissions-of-APIs-to-the-environmen-1.pdf (2018, accessed 2 November 2020).
3. de Souza SML, de Vasconcelos EC, Dziedzic M, et al. Environmental risk assessment of antibiotics: an intensive care unit analysis. *Chemosphere* 2009; 77: 962–967.
4. European Commission. *Document on risk assessment*. Technical Guidance Document on Risk Assessment Part II 337, 2003. DOI: 10.1002/mp.12308.
5. Sangion A and Gramatica P. PBT assessment and prioritization of contaminants of emerging concern: pharmaceuticals. *Environ Res* 2016; 147: 297–306.
6. Cassani S and Gramatica P. Identification of potential PBT behavior of personal care products by structural approaches. *Sustain Chem Pharm* 2015; 1: 19–27.
7. Council E. Commission directive 93/67/EEC of 20 July 1993 laying down the principles for assessment of risks to man and the environment of substances notified in accordance with council directive 67/548/EEC. *Off J Eur Commun* 1993; L227: 1–3.
8. Fent K, Weston AA and Caminada D. Ecotoxicology of human pharmaceuticals. *Aquat Toxicol* 2006; 76: 122–159.
9. Aus der Beek T, Weber F-A, Bergmann A, et al. Pharmaceuticals in the environment: global occurrence and potential cooperative action under the strategic approach to international chemicals management (SAICM), www.umweltbundesamt.de/sites/default/files/medien/1968/publikationen/iww_abschlussbericht_saicm_arzneimittel_final.pdf (2016, accessed 28 July 2020)
10. GWRC. *Pharmaceuticals and personal care products in the water cycle. An international review*. London, UK: Author, 2004.
11. Norman Network. <https://www.norman-network.net/?q=Home> (accessed 2 November 2020).
12. Petrović M, Gonzalez S and Barceló D. Analysis and removal of emerging contaminants in wastewater and drinking water. *Trends Anal Chem* 2003; 22: 685–696.
13. Monteiro S and Boxall A. Occurrence and fate of human pharmaceuticals in the environment. *Rev Environ Contam Toxicol* 2010; 202: 53–154.
14. Wojcieszynska D and Guzik U. Naproxen in the environment: its occurrence, toxicity to nontarget organisms and biodegradation. *Appl Microbiol Biotechnol* 2020; 104: 1849–1857.
15. United States Environmental Protection Agency, Toxicity Estimation Software Tool (TEST). <https://www.epa.gov/chemical-research/toxicity-estimation-software-tool-test> (2016, accessed 2 November 2020).
16. ISO 11348-3:2007(en). Water quality — determination of the inhibitory effect of water samples on the light emission of *Vibrio* Fisheri (Luminescent bacteria test) — part 3: method using freeze-dried bacteria.
17. De Vaugelade S, Nicol E, Vujovic S, et al. UV–vis degradation of α -tocopherol in a model system and in a cosmetic emulsion—structural elucidation of photoproducts and toxicological consequences. *J Chromatogr A* 2017; 1517: 126–133.
18. Naproxen Safety Data Sheet. <https://www.caymanchem.com/msdss/70290m.pdf> (accessed 2 November 2020).
19. Isidori M, Lavorgna M, Nardelli A, et al. Ecotoxicity of naproxen and its phototransformation products. *Sci Total Environ* 2005; 348: 93–101.
20. Cory WC, Welch AM, Ramirez JN, et al. Naproxen and its phototransformation products: persistence and ecotoxicity to toad tadpoles (*Anaxyrus terrestris*), individually and in mixtures. *Environ Toxicol Chem* 2019; 38: 2008–2019.
21. Kern S, Fenner K, Singer HP, et al. Identification of transformation products of organic contaminants in natural waters by computer-aided prediction and high-resolution mass spectrometry. *Environ Sci Technol* 2009; 43: 7039–7046.
22. Ternes TA. Occurrence of drugs in German sewage treatment plants and Rivers. *Water Res* 1998; 32: 3245–3260.
23. Farré ML, Ferrer I, Ginebreda A, et al. Determination of drugs in surface water and wastewater samples by liquid chromatography-mass spectrometry: methods and preliminary results including toxicity studies with *Vibrio fischeri*. *J Chromatogr A* 2001; 938: 187–197.